Macromolecules

pubs.acs.org/Macromolecules

Article

Unifying Weak and Strong Charge Correlations within the Random Phase Approximation: Polyampholytes of Various Sequences

Artem M. Rumyantsev,* Albert Johner,* Matthew V. Tirrell, and Juan J. de Pablo*

Cite This: *Macromolecules* 2022, 55, 6260−6274

Read Online

ACCESS | Metrics & More | Article Recommendations | Supporting Information

ABSTRACT: We consider the problem of charge correlations in self-coacervate phases of polyampholytes and disordered proteins with different monomer sequences. An analytical approach consistently describing both weak and strong correlations is proposed, which is based on the improvement of the random phase approximation (RPA) by taking into account (i) discreteness of charges in polymer chains and (ii) a finite number of wave modes of the charge density fluctuations. These modifications are an essential element of the particle-to-field transformation. For strong Coulomb interactions, the generalized RPA reproduces the free energy of the strongly correlated Wigner liquid of disjointed charges. The developed theory is applied to describe coil-to-globule transitions in single-chain polyampholytes as a function of the monomer sequence. Comparison with results of molecular simulations confirms that the theory reproduces the observed scaling laws for globule size at weak charge correlations, and in addition, it provides a quantitative description of electrostatic interactions when correlations are strong.

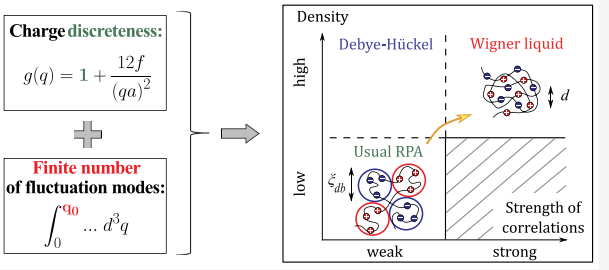

I. INTRODUCTION

Charge correlations dictate the behavior of macroscopically neutral systems of oppositely charged particles. Perhaps the simplest example is an electrolyte solution of a monovalent salt. From the statistical physics standpoint, this system is equivalent to a plasma of oppositely charged ions. For this reason, it is called the Coulomb gas or, for weak charge correlations, the Debye−Hückel plasma, referring to the authors of the seminal work[1] that introduced the concept of positional charge correlations.

The mean-field Coulomb energy of the ions, which are distributed in space homogeneously and independently from each other, is equal to zero. However, each charge is surrounded by an ionic cloud that contains more ions of opposite sign, and therefore the assembly carries a net opposite charge.[2] When interactions are weak, electrostatic attractions between the central ion and the corresponding cloud lead to a negative correlation-induced correction to the ideal-gas osmotic pressure of the Coulomb gas, but the system remains in one phase. If Coulomb interactions are strong, electrolyte solutions undergo a phase transition into an ion-rich (condensed) phase and an ion-lean phase.[3,4] Correlation effects in systems of small ions have been studied extensively for decades, particularly within the restricted primitive model[3−6] (hard-core charges spheres) and the one-component plasma model (OCP, point charges neutralized by the homogeneous background) .[7,8] They are now well understood, and excellent summaries can be found in refs 9 and 10.

In contrast, the problem of charge correlations in condensed phases of ionic polymers—the so-called complex coacervates that are formed by oppositely charged polyelectrolytes[11,12] (PEs) or self-coacervates of polyampholytes[13] (PAs)—is not fully understood. The additional complications arise because charges are connected by chemical bonds into long flexible chains. In these systems, in addition to Coulomb and excluded volume interactions, the connectivity of ionic monomers also alters positional correlations and hence the attractions between opposite charges. Another difference from simple electrolytes is that polymers have very low translational entropy, which makes them much more sensitive to any form of interaction, including electrostatic forces. For this reason, coacervates and self-coacervates readily form even when charge correlations are weak; that is, the energy of Coulomb interactions per charge is lower than the thermal energy k_BT.[11−13]

There is considerable interest in the fundamental physics of charge-driven phase separation in polymeric systems. PA self-coacervation and PE complex coacervation are considered to represent foundational models for the formation of membraneless organelles within living cells.[13−18] Statistical physics considerations for PAs have been successfully applied to describe intrinsically disordered proteins (IDPs)—unfolded proteins that undergo strong size and shape fluctuations—in

Received: March 19, 2022
Revised: June 13, 2022
Published: July 6, 2022

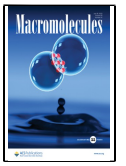

https://doi.org/10.1021/acs.macromol.2c00569
Macromolecules 2022, 55, 6260−6274

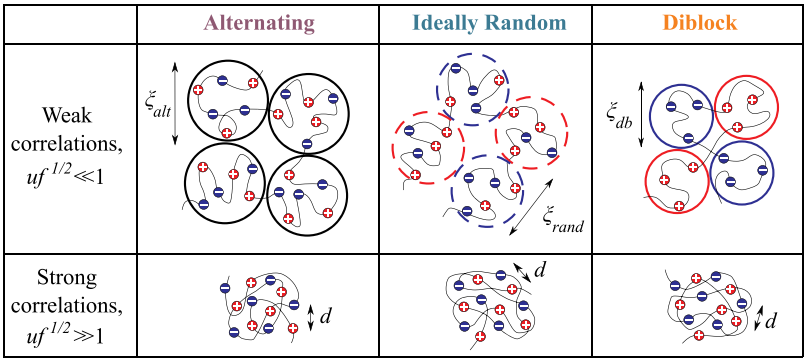

Figure 1. Blob picture of the polyampholyte globule in the regimes of weak and strong charge correlations for alternating, random, and diblock copolymer sequences. Neutral monomers are not shown explicitly and are represented by the black threads.

efforts to rationalize their phase and conformational behaviors in vitro and in vivo.[19−26]

Phase separation in solutions of IDPs is sensitive to the primary sequence of positive, negative, and neutral monomers within the molecule. Recent experiments have demonstrated that by simply varying the order in which the ionic monomers are connected, nature is capable of controlling the formation of intracellular condensates.[27] This phenomenon provides a striking manifestation of how sophisticated charge correlations in (bio)macromolecular systems can be.

The random phase approximation (RPA) became the first theoretical approach with which to explain why the high clustering of opposite charges leads to their stronger Coulomb attractions and, therefore, the propensity of charge-clustered IDPs and PAs to form self-coacervates.[19] Interestingly, this effect had been anticipated by theory[28] two decades prior to the first experimental observation. In that work, a pioneering approach (initially developed by Borue and Erukhimovich for PE complex coacervates[29,30] to calculate polymer-specific Gaussian fluctuation corrections due to Coulomb interactions) was extended to alternating and random PAs by considering their sequence-dependent charge structure factors.[28]

The RPA is based on the self-consistent calculation of pair correlation functions between ionic monomers and takes into account both their connectivity and Coulomb interactions. It is also termed the linear response approximation and represents the generalization of the Debye−Hückel theory of simple electrolytes to non-point-like objects.[29,31] The versatility of the RPA, which takes into consideration polymer architecture, stiffness, conformations,[29,32] monomer sequence,[19,22,23,25,28,33] and even orientational order,[34−36] has made it a foundational tool for description of PE complexation and PA self-coacervation. The validity of the RPA has been established through comparisons to more precise field-theoretic methods, such as renormalized Gaussian fluctuation (RGF) theory[37] and field-theoretic simulations (FTS).[22,23,38,39] RGF is the RPA modification that incorporates chain conformations in a self-consistent manner, instead of using a priori assumptions.[37,40] Numerical FTS is even more exact as it solves the field-theoretic problem by considering all (not just Gaussian) fluctuations of the polymer density fields. Both RGF and FTS have confirmed the (scaling-informed) RPA assumption for the ideal-coil statistics of flexible PEs and PAs in condensed phases under Θ solvent conditions.[37−39] Moreover, the predictions of the RPA for the density of coacervates and self-coacervates in the regime of weak correlations are consistent with the limiting power laws obtained from scaling considerations[41−45] and have been corroborated by coarse-grained simulations.[25,43,45] Finally, the RPA can be consistently refined by calculating fluctuation corrections to the mean-field pair correlation functions.[46]

An important drawback of the RPA, however, is the inability to consider strong charge correlations, which, strictly speaking, limits its applicability to weakly charged PEs and PAs, that is, molecules that contain a low fraction of ionic monomers, $f \ll 1$.[29] Synthetic polypeptides and IDPs tend to be highly charged polymers and necessitate that more sophisticated approaches be developed. In these molecules, the distance between adjacent connected charges is comparable to the monomer size along the backbone, $a \approx 0.3$ nm, which is lower than the Bjerrum length in water, $l_b = e^2/\epsilon k_B T \approx 0.7$ nm. Several methods have been proposed to describe the internal structure and charge correlations in condensed phases of ionic polymers with $f \approx 1$.

Perry and Sing developed a PRISM-based theory of homoPE coacervation that incorporates charge connectivity into the standard liquid state theory (LST) machinery, which relies on the Ornstein−Zernike equations.[47] The PRISM theory, however, requires numerical solution of the underlying integral equations, which limits the tractability of the overall approach.

Building on Blum's original works,[48,49] Wang et al. proposed another LST-based approach that provides a closed-form expression for the correlation free energy. Specifically, these authors combined the mean spherical approximation (MSA) for disjointed ions with the perturbation correction responsible for chain connectivity.[50−52] The resulting formalism provides a good description of dense coacervates with strong correlations. Improvements are needed for weak correlations, where the theory does not reproduce the limiting power law for polymer concentration. (Note that the same applies to the transfer matrix theory of complex coacervation, which neglects the conformational statistics of PEs.[53]) In its current form, this LST-based method does not consider the role of monomer sequences.

More generally, an important body of work has sought to describe strong charge correlations within various models of ion pairing[54−59] or the adsorption of one chain onto another.[53] This approach is better suited for weakly charged systems, $f \ll 1$, where Coulomb correlations can be viewed as effectively pairwise; for highly charged polymers, Coulomb interactions are inherently many-body, as discussed below.

The above summary underscores the need for a general theory that retains all the advantages of the RPA for the description of weak charge correlations and that is also capable

https://doi.org/10.1021/acs.macromol.2c00569
Macromolecules 2022, 55, 6260−6274

of describing strong correlations. In this work, by generalizing the RPA to the latter case and actually to any correlations strength, we present the unifying theory describing Coulomb interactions in condensed phases of ionic polymers. To demonstrate the advantages of the proposed approach, it is applied to compare the behaviors of alternating, ideally random, and diblock PAs in a wide range of Coulomb interaction strengths.

This paper is organized as follows. Section II is devoted to a scaling analysis of weak and strong charge correlations in self-coacervates and globules of sequence-specific PAs. Section III presents the derivation of the closed-form results for the generalized RPA (GRPA) free energies and discusses their consistency with the scaling analysis. In section IV we apply the proposed framework to describe the sequence-dependent collapse of single-chain PAs. Our theoretical results are then compared to those of molecular simulations in section V. Section VI summarizes our main conclusions.

II. SCALING ARGUMENTS

II.1. Regime of Weak Charge Correlations. In a Θ solvent, Coulomb attractions between charges of opposite sign cause long globally neutral PAs of arbitrary monomer sequence to form globules. In the regime of weak charge correlations, their internal structure is strongly sequence-dependent, as illustrated in the top panel of Figure 1. Recent works[25,26] have examined the scaling laws for globule densities and correlation lengths within them. We briefly revisit the particular cases of alternating, random, and diblock PA carrying a fraction f of equidistant ionic monomers, which are assumed to be pH-independent. Chains are flexible, and the statistical segment containing one monomer has length a. The concentration of monomers within the globule is expressed in $1/a^3$ units and is denoted by ϕ; up to a numerical coefficient, it coincides with the polymer volume fraction.

In alternating PAs, Coulomb interactions are reduced to effectively short-range dipole−dipole attractions between the pairs of adjacent positive and negative charges. Two dipoles with moments $p \simeq eaf^{-1/2}$ interact via a Keesom potential $W_K \simeq -l_b^2 p^4/r^6$ (all energies are expressed in k_BT units), which enables direct calculation of the second virial coefficient,[25,60] $B_{dip} \simeq -a^3u^2f^{-1/2}$, with $u = l_b/a$. The energy of pairwise dipole−dipole attractions per blob, given by $F_{dip} \simeq \xi_{alt}^{-3}B_{dip}(f\phi_{alt})^2$, is equal to the thermal energy k_BT. Using the closure between the correlation length (blob size) and the globule density provided by ideal-coil chain statistics in Θ solvent, $\xi \simeq a\phi^{-1}$, one finds

$$\phi_{alt} \simeq u^2 f^{3/2} \tag{1}$$

$$\xi_{alt} \simeq au^{-2}f^{-3/2} \tag{2}$$

Blobs within a globule of an alternating PA are electroneutral and contain $g_{alt} \simeq (\xi_{alt}/a)^2 \simeq u^{-4}f^{-3}$ monomers, that is, $fg_{alt} \simeq u^{-4}f^{-2}$ charges. The requirement of weak charge correlations implies that the energy of Coulomb interactions per charge is much lower than the thermal energy, $fg_{alt} \gg 1$. It can be written as $uf^{1/2} \ll 1$.

The globules formed by ideally random PAs are stabilized by bare Coulomb attractions between oppositely charged neighboring blobs. Their characteristic charge $q_{rand} \simeq e(fg_{rand})^{1/2}$ is provided by the statistical deviation from the average zero value. The balance between Coulomb attractions and three-body repulsions, written as $F_{Coul} \simeq q_{rand}^2/\epsilon\xi_{rand}k_BT \simeq 1$, yields

$$\phi_{rand} \simeq uf \tag{3}$$

$$\xi_{rand} \simeq au^{-1}f^{-1} \tag{4}$$

and $g_{rand} \simeq u^{-2}f^{-2}$. These results had been first obtained by Higgs and Joanny,[61] and the corresponding scaling picture was later proposed by Dobrynin et al.[41] They hold as long as charge correlations are weak, $fg_{rand} \gg 1$ or, equivalently, $uf^{1/2} \ll 1$.

The internal structure of a diblock PA globule can be viewed as a melt of oppositely charged electrostatic blobs, each of size $\xi_e \simeq au^{-1/3}f^{-2/3}$ and carrying charge $q_e \simeq ef\xi_e^2 \simeq eu^{-2/3}f^{-1/3}$. It is analogous to that of a charge-symmetric polyelectrolyte complex coacervate.[39,42,44,45,62] The balance between long-range Coulomb attractions and short-range three-body repulsions is provided by $q_e^2/\epsilon\xi_e k_BT \simeq 1$. The resulting globule properties are given by

$$\phi_{db} \simeq (uf^2)^{1/3} \tag{5}$$

$$\xi_{db} \simeq \xi_e \simeq a(uf^2)^{-1/3} \tag{6}$$

and $g_{db} \simeq (uf^2)^{-2/3}$. The number of ionic monomers within the blob fg_{db} is high, and charge correlations are weak provided that $uf^{1/2} \ll 1$.

II.2. Regime of Strong Charge Correlations. We emphasize that the crossover between the regimes of weak and strong charge correlations is universal for all types of sequences, and is given by[59,63]

$$uf^{1/2} \simeq 1 \tag{7}$$

At the crossover, each concentration blob within the globule contains on the order of one charge. Therefore, at $uf^{1/2} \gg 1$, in the regime of strong charge correlations, there is on average less than one charge per concentration blob. In this case, charge correlations within the globule are not affected by the sequence of ionic monomers in the PA. One can compare the distance between two consecutive ionic monomers along the chain, $R_f \simeq af^{-1/2}$, and the concentration blob size ξ, which are equal at the crossover. In the regime of strong charge correlations, the former is higher, $R_f \gg \xi$. That is, at $uf^{1/2} \gg 1$, the nearest-neighbor charges *along the chain* are not the *spatially* closest charges. This observation clarifies why charge correlations—and the resulting structure and dimensions of the PA globules—become sequence-independent when charge correlations are sufficiently strong. The bottom panel in Figure 1 illustrates the internal structure of these globules.

Irrespective of the monomer sequence, each charged monomer within a *homogeneous* PA globule is preferentially surrounded by its oppositely charged counterparts. The energy of Coulomb attractions per charge (in k_BT units) can be estimated as

$$W \simeq -\frac{e^2}{\epsilon d k_B T} \simeq -\frac{l_b}{d} \tag{8}$$

Here the distance d between the most spatially proximal charges is a function of the globule density.

$$d \simeq a(f\phi)^{-1/3} \tag{9}$$

The free energy density of Coulomb interactions (expressed in units of k_BT/a^3) is therefore given by

https://doi.org/10.1021/acs.macromol.2c00569
Macromolecules 2022, 55, 6260−6274

$$F_{SC} = f\phi W \simeq -u(f\phi)^{4/3} \tag{10}$$

This result is well-known for homogeneous systems of strongly correlated pointlike charges and is often termed the correlation free energy of the strongly correlated "Wigner liquid" (WL) or of the OCP.[9,63−66] At very high u values one expects the formation of the ionic (Wigner) crystal. We limit our considerations to the liquid (amorphous) state but note that in the presence of the long-range order the scaling result given by eq 10 remains valid and is usually termed the Madelung energy,[67] with a numerical prefactor defined by the type of crystalline lattice.

Equation 10 is the key result of a scaling analysis. By combining it with the free energy for three-body repulsions, $F_{vol} \simeq \phi^3$, one can find the globule density, $\phi_{SC} \simeq u^{3/5}f^{4/5}$.[63,68] However, this power law does not hold over a broad range of parameters because of the high globule density in the regime of strong correlations and is difficult to attain in experiments or simulations, which actually reveal $\phi \sim f^{0.4}$ for $f \geq 0.5$.[69] Already at the crossover for weak and strong correlations, $uf^{1/2} \simeq 1$, the density is high, $\phi \simeq f^{1/2}$, because f cannot be very low without violating the assumption of internal globule homogeneity (see item i below). This makes the virial expansion form of F_{vol} inapplicable, and one should instead use the Flory−Huggins free energy with $\chi = 1/2$ corresponding to the Θ solvent conditions or the modified Carnahan−Starling expression.

II.3. Discussion. There are several important remarks to be made on the obtained scaling results:

(i) The picture of strong correlations outlined above holds for a homogeneous globule, which is the case for sufficiently high f values. In this respect, fully charged PAs, $f = 1$, represent a limiting case. In contrast, for low fractions of ionic monomers, $f \ll 1$, one expects the formation of finite-size clusters rich in ionic monomers. This is confirmed by molecular dynamics simulations, where chains collapse into microstructured globules containing single ion pairs or aggregates (dense ionomer domains) surrounded by more swollen loops of neutral monomers.[43] Several theoretical models are available to describe aggregate formation in the context of ionomer melts,[70−72] polyelectrolyte solutions/gels,[73−75] and complex coacervates.[59] A detailed analysis of the instability of a homogeneous globule with respect to this type of microphase separation at decreasing f and/or increasing u is beyond the scope of this work and requires additional considerations.

(ii) From a theoretical point of view, the approach described above for strong charge correlations differs from those that have considered the association of charges into ion pairs[54−59,76−78] and further into multiplets.[73−75] The energy gain ΔE_{ip} due to the formation of the contact ion pair with *the fixed distance between the ions* is always assumed to be independent of polymer concentration. Therefore, when charge attractions are strong and almost all ions associate, ion-pairing models predict the free energy density of Coulomb interactions to be[54−59,73−78]

$$F_{SC} \simeq f\phi\Delta E_{ip} \tag{11}$$

This result is linear in ϕ and differs from eq 10, suggesting that $F_{SC} \sim -\phi^{4/3}$. Approaches based on ion pairing are better suited for weakly charged PAs and PEs containing a small fraction of ionic monomers, $f \ll 1$.[54,55,59,73−76] In this case, one can assume that ΔE_{ip} is independent of ϕ for a single isolated ion pair. However, for strongly charged polymers with $f \simeq 1$, each charge is surrounded by *numerous* opposite and even charges. These *collective* Coulomb interactions cannot be reduced to effective pairwise, saturating ion associations, and for that reason, our proposed approach to strong correlations (as well as the LST route[47,50−52]) would appear to be better justified for highly charged PAs and PEs than ion-pairing frameworks.

The suitability of these two approaches depends on the microscopic (chemical) structure of ionic monomers. The concept of ion pairing is expected to work better for PEs and PAs that carry compact ionic groups at the end of long side chains, while interactions of bulky charges located near or along the backbone are better described as collective interactions. The second method should be also better applicable to the standard coarse-grained simulation models, with the electric charge placed in the center of the bead.[79]

(iii) The scaling regimes outlined above correspond to the limiting cases of weak and strong charge correlations, and the crossover between them is relatively wide. The latter is exemplified by the ratio $\phi_{SC}/\phi_{db} \simeq (uf^{1/2})^{4/15}$, which increases slowly with u. Perhaps the most interesting case of strongly charged PEs and PAs in aqueous solution corresponds to $f = 1$ and $u \approx 1-3$, depending on backbone chemistry, and therefore belongs to the crossover region. This underscores the need for a field-theoretic approach that quantitatively and accurately describes charge correlations over the entire range of their strength. This challenge is addressed in the following section.

III. RANDOM PHASE APPROXIMATION

III.1. Derivation of Unifying Closed-Form Results. The mean-field free energy of Coulomb interactions within globally neutral PA globules is zero. The random phase approximation (RPA) provides Gaussian corrections to the mean-field result; pairwise correlation functions are calculated at the mean-field level. The inverse charge structure factor of the PA solution (i.e., the globule interior) is written as the sum of the inverse charge structure factor of noninteracting chains and the contribution due to Coulomb interactions of charges:[19,25,28]

$$G^{-1}(q) = G_0^{-1}(q) + U(q) = G_0^{-1}(q) + \frac{4\pi u}{(qa)^2} \tag{12}$$

Owing to the ideal-coil statistics of PAs under Θ solvent conditions, the first contribution can be written as[25,28]

$$G_0(q) = f\phi g_\lambda(q) = f\phi\frac{1 + \lambda e^{-(qa)^2/6f}}{1 - \lambda e^{-(qa)^2/6f}} \tag{13}$$

with $\lambda = -1$, 0, and 1 corresponding to alternating, ideally random, and diblock PAs.[25] Chains are assumed to be infinitely long, $N \to \infty$.

To arrive at the analytical results for the RPA free energy correction, the single-chain charge structure factors of alternating and diblock PAs are approximated as follows:

$$g_{alt}(q) \approx \frac{(qa)^2}{12f + (qa)^2} \tag{14}$$

$$g_{rand}(q) = 1 \tag{15}$$

$$g_{db}(q) \approx 1 + \frac{12f}{(qa)^2} \tag{16}$$

These results are derived by assuming ideal-coil chain conformations at all length scales. While at the lengths larger

https://doi.org/10.1021/acs.macromol.2c00569
Macromolecules 2022, 55, 6260−6274

than the blob size this is the case for any solvent quality,[44] Gaussian statistics within the blob is provided by Θ solvent conditions. We emphasize that the form adopted here for the structure factors takes into account the pointlike nature of charges in PA chains:[77,82] For any sequence, $g_\lambda(q) \to 1$ and $G_0(q) \to f\phi$ at $q \to \infty$, where $f\phi$ is the density of charges in the system. This first aspect of the RPA calculations is critical for the generalization to the regime of strong charge correlations.

The second key aspect of our approach is to introduce a cutoff in the RPA integration over the fluctuation wave modes in a manner that considers only physically meaningful fluctuations of *the charge density field*:

$$F_{RPA} = \frac{a^3}{2}\int_0^{q_0} \frac{d^3q}{(2\pi)^3} \ln\left(\frac{G^{-1}(q)}{G_0^{-1}(q)}\right) - F_{self} = \frac{a^3}{2}\int_0^{q_0} \frac{d^3q}{(2\pi)^3}\left[\ln\left(1 + \frac{g_\lambda(q)}{(r_D q)^2}\right) - \frac{g_\lambda(q)}{(r_D q)^2}\right] \quad (17)$$

Here $r_D = (4\pi u f\phi)^{-1/2}a$ is the Debye length for the system of disjointed charges and F_{self} is the self-energy of the PA.[40,83] The integration cutoff idea has its roots in the classical work by Debye on the heat capacity of solids,[2,84,85] where Einstein's calculations were improved and the well-known $C_v \sim T^3$ law for the low-temperature region was derived. The minimal wavelength of the (charge) density fluctuations cannot be lower than the distance d between the nearest (charged) particles—atoms in solids or charged monomers in the present problem. Therefore, the q-integration should be performed over $q \le q_0$ with

$$q_0 \simeq d^{-1} \simeq (f\phi)^{1/3}a^{-1} \quad (18)$$

This adaptation of Debye's idea to calculations of the correlation free energy in ionic systems was first proposed in the context of a non-Debye, strongly correlated plasma[86] and later applied to various ionic systems.[64,77,87−89] Following Brilliantov,[64,88] the cutoff value q_0 can be found by calculating the total number of fluctuation modes in a system of volume V containing $\mathcal{N} = f\phi V/a^3$ particles:

$$2\frac{V}{(2\pi)^3}\int_0^{q_0} 4\pi q^2\, dq = 3\mathcal{N} \quad (19)$$

The numerical coefficient on the left-hand side of this equation is due to two (sine and cosine) fluctuation modes corresponding to the same **q** vector, while that on the right-hand side takes into account that there are three translational degrees of freedom per charge. The latter depends on the microscopic model of the PAs and would be lower if the ionic monomers were connected by stiff bonds of fixed length, as opposed to flexible Gaussian or harmonic springs. Equation 19 leads to a cutoff wavevector given by[64]

$$q_0 = (9\pi^2 f\phi)^{1/3}a^{-1} \quad (20)$$

A similar value of q_0 was reported by Bohm and Pines in their seminal work on the degenerate electron gas, where the RPA method was first introduced.[90] The idea of the RPA integration cutoff has appeared before in the PE literature in the context of semidilute solutions,[77] albeit the physical motivation in that work was somewhat different.[91] To recapitulate, the integration cutoff adopted here is not an ad hoc ansatz but represents a fundamental physical aspect of the particle-based problem, which is important for arriving at a correct representation in terms of fluctuating fields.

The final results for the RPA correlation free energies given by eq 17 can be found analytically for all three sequences considered here. For alternating sequences, $\lambda = -1$, one can find

$$F_{RPA}^{alt} = \frac{1}{12\pi^2(r_D/a)^3}\left[t_0^3 \ln\left(1 + \frac{1}{t_0^2 + s^{-2}}\right) - t_0 + s^{-1}(3 + 2s^{-2})\arctan(st_0) - 2(1 + s^{-2})^{3/2} \times \arctan\left(\frac{t_0}{\sqrt{1 + s^{-2}}}\right)\right] \quad (21)$$

where

$$t_0 = r_D q_0; \quad s = \frac{r_p^2}{r_D^2} = \frac{R_f}{r_D} = \sqrt{\frac{\pi u\phi}{3}} \quad (22)$$

Here $r_p = (48\pi u f^2\phi)^{-1/4}a$ is the polymer screening radius, and $R_f = (12f)^{-1/2}a$ the distance between adjacent charges along the chain.[28−30] For $f = 1$, eq 21 is similar to the correlation energy recently reported for polyzwitterions with monomer dipole moments perpendicular to the chain backbone.[89]

For ideally random PAs, $\lambda = 0$, our result coincides with that reported by Brilliantov for OCP:[64]

$$F_{RPA}^{rand} = \frac{1}{12\pi^2(r_D/a)^3}\left[t_0^3 \ln\left(1 + \frac{1}{t_0^2}\right) - t_0 - 2\arctan(t_0)\right] \quad (23)$$

Finally, the correlation free energy for diblock PAs, $\lambda \to 1$, is given by

$$F_{RPA}^{db} = \frac{1}{12\pi^2(r_D/a)^3}\left[t_0^3 \ln\left(1 + \frac{1}{t_0^2} + \frac{1}{s^2 t_0^4}\right) - t_0 + \frac{3}{s^2 t_0} - \frac{(1-\varkappa)^{3/2}}{\sqrt{2}}\arctan\left(\frac{\sqrt{2}\,t_0}{\sqrt{1-\varkappa}}\right) - \frac{(1+\varkappa)^{3/2}}{\sqrt{2}} \times \arctan\left(\frac{\sqrt{2}\,t_0}{\sqrt{1+\varkappa}}\right)\right] \quad (24)$$

with $\varkappa^2 = 1 - 4\ s^{-2}$. In eq 24, the term linear in ϕ is physically irrelevant and has been omitted.[92]

Equations 21, 23, and 24 are the main results of our work. They are equally applicable to macroscopic self-coacervate phases of PAs and to the interior of the PA globules. Moreover, eq 24 is valid for symmetric PE complex coacervates. Below we demonstrate that these results unify the regimes of weak and strong charge correlations.

The strength of Coulomb interactions and charge correlations is controlled by the dimensionless parameter $t_0 = q_0 r_D = 1.598\Gamma^{-1/2}$, which is closely related to the Coulomb coupling parameter[9,64,66]

$$\Gamma = \left(\frac{4\pi}{3}\right)^{1/3} u(f\phi)^{1/3} \simeq \frac{l_b}{d} \quad (25)$$

Γ is equal to the ratio between the Coulomb energy of the charge and the thermal energy k_BT, $\Gamma \simeq |W|$ (see eq 8). Therefore, $t_0 \gg 1$ ($\Gamma \ll 1$) and $t_0 \ll 1$ ($\Gamma \gg 1$) describe the

https://doi.org/10.1021/acs.macromol.2c00569
Macromolecules 2022, 55, 6260−6274

regimes of weak and strong correlations, respectively. Figure 2 summarizes the regimes of charge correlations predicted here.

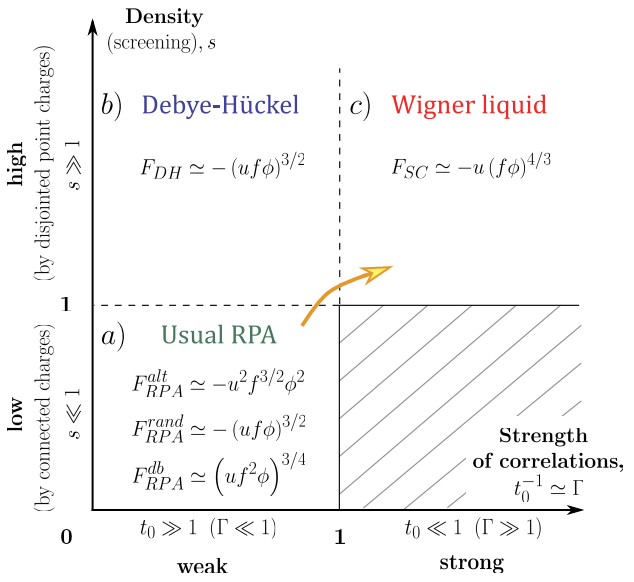

Figure 2. Scaling regimes of charge correlations in polyampholyte self-coacervates/globules and correlation free energy densities predicted within the generalized RPA: (a) results of the standard RPA for low densities and weak correlations; (b) Debye−Hückel law for high densities and weak correlations; (c) Wigner liquid scaling for dense systems with strong correlations. The shaded area corresponds to a nonphysical range of parameters. The arrow illustrates the evolution of the system with increasing u.

III.2. Regime of Weak Charge Correlations.

For weak charge correlations, $t_0 \gg 1$ ($\Gamma \ll 1$), our results coincide with those of the standard RPA without the integration cutoff:[29,30]

$$F_{\mathrm{RPA}}^{\mathrm{alt}} = -\frac{1}{12\pi(r_{\mathrm{D}}/a)^3}[(1+s^{-2})^{3/2} - s^{-3}] \tag{26}$$

$$F_{\mathrm{RPA}}^{\mathrm{rand}} = -\frac{1}{12\pi(r_{\mathrm{D}}/a)^3} = -\frac{2\sqrt{\pi}}{3}(uf\phi)^{3/2} \tag{27}$$

$$F_{\mathrm{RPA}}^{\mathrm{db}} = \frac{1}{12\pi(r_{\mathrm{p}}/a)^3}(1-s)\sqrt{2+s} \tag{28}$$

The parameter s defines the density regime of the system as well as the charge screening regime,[29] as seen from eq 22. If charge correlations are weak, the equilibrium densities of PA globules in a Θ solvent are low, $s \ll 1$. In this case, the correlation free energies for alternating and diblock PAs are given by

$$F_{\mathrm{RPA}}^{\mathrm{alt}} \approx -\frac{\pi}{4\sqrt{3}}u^2 f^{3/2}\phi^2 \tag{29}$$

$$F_{\mathrm{RPA}}^{\mathrm{db}} \approx \frac{(48\pi)^{3/4}}{6\sqrt{2}\,\pi}(uf^2\phi)^{3/4} \tag{30}$$

where the term linear in ϕ in eq 29 (the self-energy of dipoles) has been omitted. Combining the results above for the correlation free energies with the three-body repulsive contribution, $F_{\mathrm{vol}} = w\phi^3$, we arrive at the equilibrium globule densities in the regime of weak correlations

$$\phi_{\mathrm{alt}} = \frac{\pi}{8\sqrt{3}}u^2 f^{3/2} w^{-1} \tag{31}$$

$$\phi_{\mathrm{rand}} = \left(\frac{\pi}{36}\right)^{1/3} ufw^{-2/3} \tag{32}$$

$$\phi_{\mathrm{db}} = \frac{1}{2^{2/3}(3\pi)^{1/9}}(uf^2)^{1/3} w^{-4/9} \tag{33}$$

They are consistent with the scaling results given by eqs 1, 3, and 5.[25] The numerical coefficient in ϕ_{alt} differs slightly from that reported earlier[25,28,93] because of the approximation adopted here for the charge structure factor g_{alt}. One can also confirm that the low density requirement, $s \ll 1$, is fulfilled provided that charge correlations are weak, $t_0 \gg 1$.

Finally, for weak charge correlations and high polymer densities, $t_0 \gg 1$ and $s \gg 1$ (see Figure 2), the RPA correlation free energy is sequence-independent and reduces to the Debye−Hückel result given by eq 27 for any PA.[82] This regime does not arise for equilibrium PA globules in a Θ solvent and can only be realized if the globule is compressed by external forces or if a high polymer concentration is created by the non-Coulomb attractions between monomers (e.g., poor solvent conditions).

III.3. Regime of Strong Charge Correlations.

At $t_0 \ll 1$ ($\Gamma \gg 1$), charge correlations are strong and the system is therefore dense, $st_0 \gtrsim 1$. The latter condition demonstrates that adjacent charges along the chain are no longer the only nearest spatial neighbors of a given charge, $R_{\mathrm{f}} \gtrsim d$. In the asymptotic limit of $st_0 \gg 1$, when the closest connected charges cease to be the nearest spatial neighbors, $R_{\mathrm{f}} \gg d$, the RPA correlation free energies are independent of the PA sequence:

$$F_{\mathrm{RPA}}^{\mathrm{alt}} = F_{\mathrm{RPA}}^{\mathrm{rand}} = F_{\mathrm{RPA}}^{\mathrm{db}} = F_{\mathrm{RPA}}^{\mathrm{SC}} = -\left(\frac{9}{\pi}\right)^{1/3} u(f\phi)^{4/3} \tag{34}$$

Equation 34 is consistent with the scaling estimate given by eq 10 and the microscopic picture of the charge spacing at $R_{\mathrm{f}} \gg d$ shown in Figure 1.

The limit of $st_0 \gg 1$ and $R_{\mathrm{f}} \gg d$ cannot occur for highly charged PAs with $f \simeq 1$, which represent the primary interest of this work, particularly in the context of strong correlations. Fully charged PAs at high Bjerrum lengths are expected to exhibit $R_{\mathrm{f}} \simeq d$ and $st_0 \simeq 1$. According to the scaling picture of dense PA globules shown in Figure 1, the WL behavior should remain valid at the $R_{\mathrm{f}} \simeq d$ crossover, when each charge is surrounded by many other charges (the coordination number for a 3D liquid of spheres is ≃10), with just two of them connected by a chemical bond. If that is the case, the question arises: why is the requirement of $R_{\mathrm{f}} \gg d$ necessary to obtain the asymptotic eq 34 from the general RPA results, eqs 21 and 23−24?

The answer is provided by the different reference levels (states) with respect to which the energy of Coulomb interactions is calculated within the RPA and the scaling approaches. Scaling estimates of eqs 8−10 implicitly assume that the ground level is the system of *disjointed* point charges at infinite distance. For the RPA calculations, the reference state depends on the self-energy subtraction and, according to eq 17, corresponds to the point charges *already connected* by Gaussian threads (chemical bonds) into single PA chains located far from each other.[40,83] In the presence of the q cutoff, when (the term corresponding to) the self-energy of PA chains becomes nonlinear in ϕ and therefore relevant for thermodynamics, this

https://doi.org/10.1021/acs.macromol.2c00569
Macromolecules 2022, 55, 6260−6274

choice of the ground state, provided by $F_{self} = F_{self}^{PA}$, is necessary to properly describe Coulomb attractions between opposite charges and the resulting collapse of PAs. Thus, F_{RPA} does not account for 1−2, 1−3, and further electrostatic interactions along the chain and does not reproduce WL scaling without fulfilling the condition that $R_f \gg d$.

Nevertheless, substituting the subtracted self-energy of PAs with that of the point charges in eq 17

$$F_{self}^{PA} = \frac{a^3}{2}\int_0^{q_0}\frac{d^3q}{(2\pi)^3}\frac{g_\lambda(q)}{(r_D q)^2}\ldots \rightarrow F_{self}^{pc} = \frac{a^3}{2}\int_0^{q_0}\frac{d^3q}{(2\pi)^3}\frac{1}{(r_D q)^2} \tag{35}$$

allows us to change the reference energy level and obtain $\tilde{F}_{RPA}$, thereby satisfying WL scaling, eq 34, without the requirement that $R_f \gg d$ ($st_0 \gg 1$). In contrast to F_{RPA}, the renormalized $\tilde{F}_{RPA}$ takes into account electrostatic interactions between all connected charges, including those between the nearest bonded monomers. For ideally random PAs, charge statistics provide a zero self-energy for their connectivity and $F_{RPA}^{rand} = \tilde{F}_{RPA}^{rand}$. For alternating PAs, $\tilde{F}_{RPA}^{alt}$ is given by eq 21 without the 3 $s^{-1}\arctan(st_0)$ term in the brackets. For diblock PA, $\tilde{F}_{RPA}^{db}$ can be obtained from eq 24 by canceling the $3/s^2t_0$ contribution in the brackets because the latter arises from the integration of the connectivity-related part of the diblock PA structure factor, $g_{db}(q) - 1 = 12f/(qa)^2$. We emphasize that F_{RPA}, rather than $\tilde{F}_{RPA}$, should be used to find the equilibrium globule density ϕ; after ϕ is obtained, the calculated $\tilde{F}_{RPA}$ represents the energy of Coulomb interactions between all ionic monomers in the system and can be compared to that obtained directly from simulations.

Finally, it should be noted that the case of strong charge correlations, $t_0 \ll 1$, and simultaneously low densities, $st_0 \ll 1$ ($R_f \ll d$), seems unphysical and is not considered here. It corresponds to an unstable configurations of charges, which interact strongly but do not approach each other closely.

III.4. Comparison to the Mean Spherical Approximation (MSA). The MSA is the classical approximation in the LST, which extends the DH theory of simple electrolytes from weak to strong Coulomb interactions. The MSA provides the correlation free energy of the restricted primitive model of simple electrolytes (disjointed charged hard spheres) in analytical form:[5,6]

$$F_{MSA} = -\frac{1}{12\pi(\sigma/a)^3}[3x^2 + 6x + 2 - 2(1+2x)^{3/2}] \tag{36}$$

Here σ is the diameter of ions, and $x = \sigma/r_D$ is the ratio of the ion diameter to the Debye length. The MSA[50−52] (and related LST approaches[47]) have been recently used to describe strong charge correlations in fully charged PE complexes and PAs with $f = 1$. It is of interest to compare the results of the improved RPA and the MSA. In the regime of weak charge correlations, $r_D/d \gg 1$ and therefore $x \rightarrow 0$, the MSA reproduces the DH correction for disjointed charges, $F_{MSA}^{WC} \approx -a^3/12\pi r_D^3$. For strong charge correlations, $r_D/d \ll 1$ and therefore $x \rightarrow \infty$, the leading contribution is given by

$$F_{MSA}^{SC} \approx -\frac{l_b}{\sigma}\phi \tag{37}$$

This asymptotic result predicts a slightly different power-law dependence on ϕ as compared to eq 10, $F_{SC} \sim \phi$ versus $F_{SC} \sim \phi^{4/3}$ (ion pairing scaling versus Wigner liquid scaling). However, we note that the basic MSA assumption is that ions are treated as charged hard spheres interacting via the following pairwise potential

$$v_{ij}(r) = \begin{cases} \infty, & r < \sigma \\ \dfrac{z_i z_j}{\epsilon r}, & r > \sigma \end{cases} \tag{38}$$

This form of $v_{ij}(r)$ suggests that when charge correlations are very strong and the system is almost incompressible, the concentration of ions and ionic size are coupled through $\phi\sigma^3/a^3 \simeq 1$. Using this relationship, one arrives at

$$F_{MSA}^{SC} = -u\phi^{4/3} \tag{39}$$

which is consistent with our result and WL scaling.

The similarity between the MSA and the generalized RPA stems from the linearity of both approaches. Within the MSA, the closure between the pairwise potentials and direct correlation functions is given by $c_{ij}(r) = -v_{ij}/k_BT$ for $r > \sigma$. The interaction-induced contribution to the RPA correlation functions, which is defined by the second term in eq 12, is identical. Moreover, the q cutoff introduced into the generalized RPA virtually implies that the system is locally incompressible, $c_{ij}(r) \approx 0$ for $r \lesssim q_0^{-1} \simeq d$, because no integration over these short-wavelength fluctuations is performed. When the system is so dense that the dependence of q_0 on ϕ is negligible and $d \simeq \sigma$, this coincides with the MSA closure approximation for short distances, $c_{ij}(r) = 0$ for $r < \sigma$. In a similar way, Ermoshkin and Olvera de la Cruz have argued earlier that introducing the ϕ-independent integration cutoff to the RPA, $\tilde{q}_0 \simeq \sigma^{-1}$, can be used to account for the hard-sphere nature of monomers.[77] Using this hard-core cutoff would yield $F_{SC} \simeq -uf\phi$ scaling for the RPA correlation free energy, which exactly coincides with the MSA, as demonstrated in the Supporting Information. In contrast, using the concentration-dependent cutoff $q_0 \simeq d^{-1} \simeq a^{-1}(f\phi)^{1/3}$ results in $F_{SC} \simeq -u(f\phi)^{4/3}$. We, however, emphasize that the latter cutoff, which is defined by eq 20, has more rigorous and universal physical grounds, as discussed earlier. It is not limited to the hard-sphere case and is applicable to more realistic systems with arbitrary repulsive parts of the pairwise interaction potentials. Recall that the MSA indeed exhibits some artifacts caused by hard-sphere interactions, which can be eliminated if the repulsion is softened.[10]

The key advantage of the improved RPA over the MSA is that it accounts for charge connectivity in a reasonable manner, which is crucial in the weak correlations regime. Additionally, the generalized RPA is not limited to $f = 1$.

III.5. Applicability Range of the Generalized RPA. The RPA is applicable to concentrated homogeneous systems with weak density fluctuations.[80,81] It is therefore expected that the generalized RPA is valid in the regimes of both weak and strong correlations. To rigorously demonstrate that, the next order term $F^{(3)}$ should be compared with the calculated Gaussian correction. The former is given by[29]

$$F^{(3)} \simeq a^6\int_0^{q_0}[\Gamma^{(3)}(q_1, q_2, q_3)]^2 G(q_1)G(q_2)G(q_3) \times \delta(\mathbf{q}_1 + \mathbf{q}_2 + \mathbf{q}_3)\, d^3q_1\, d^3q_2\, d^3q_3 \tag{40}$$

where $\Gamma^{(3)}(q_1,q_2,q_3)$ is the third-order vertex function, $G(q)$ is given by eq 12, and the same integration cutoff has been introduced as that used for the second-order term calculations.

https://doi.org/10.1021/acs.macromol.2c00569
Macromolecules 2022, 55, 6260−6274

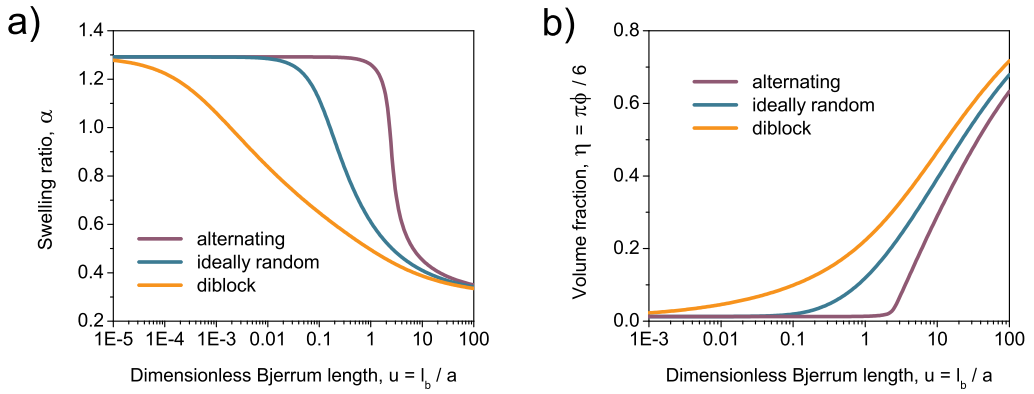

Figure 3. Collapse of alternating, random, and diblock PAs induced by Coulomb interactions under Θ solvent conditions: (a) swelling ratio α of PAs and (b) polymer volume fraction η within them as functions of the dimensionless Bjerrum length, $u = l_b/a$. PAs are fully charged, $f = 1$, and consist of $N = 10^3$ monomers. A comparison of these results with those obtained within the standard RPA is performed in the Supporting Information.

The RPA's validity has been established when charge correlations are weak.[29,46] To illustrate this, consider ideally random PAs with $\Gamma^{(3)}_{\text{rand}}(q) \simeq (f\phi)^{-2}$ and $G_{\text{rand}}(q) = f\phi/(1 + r_D^{-2}q^{-2})$. Neglecting the integration cutoff, one can obtain the estimate $F^{(3)}_{\text{rand}} \simeq a^6/f\phi r_D^6$ and find that the perturbation theory parameter (PTP) is small

$$\text{PTP}_{\text{WC}} = \frac{F^{(3)}_{\text{rand}}}{F^{\text{rand}}_{\text{RPA}}} \simeq \frac{a^3}{f\phi r_D^3} \simeq \frac{l_b}{r_D} \simeq \left(\frac{d}{r_D}\right)^3 \simeq \left(\frac{l_b}{d}\right)^{3/2} \ll 1 \tag{41}$$

provided that $d \gg l_b$. This constraint is nothing but the requirement of weak correlations, which, under Θ solvent conditions, reads $uf^{1/2} \ll 1$.

If charge correlations are strong, and an integration cutoff is essential, $t_0 \ll 1$, the next order correction is given by $F^{(3)}_{\text{rand}} \simeq (ar_Dq_0^2)^6/f\phi \simeq (q_0a)^3t_0^6$, which is independent of the PA's sequence. The validity of the RPA

$$\text{PTP}_{\text{SC}} = \frac{F^{(3)}_{\text{rand}}}{F^{\text{rand}}_{\text{RPA}}} \simeq \frac{(q_0a)^3t_0^6}{u(f\phi)^{4/3}} \simeq \left(\frac{r_D}{l_b}\right)^{8/3} \simeq \left(\frac{r_D}{d}\right)^8 \simeq \left(\frac{d}{l_b}\right)^4 \ll 1 \tag{42}$$

is now provided by $d \ll l_b$, satisfied in the regime of strong correlations. This conclusion is consistent with the detailed analysis of ref 87 serving to demonstrate that for strongly correlated OCP higher-order corrections to the improved RPA term are essentially negligible.

The discussion above underscores that the improved RPA is rigorous and asymptotically exact for both weak and strong correlations. Using the integration cutoff due to hard-core repulsions between monomers, $\tilde{q}_0 \simeq a^{-1}$, instead of that due to a finite number of fluctuation wave modes, $q_0 \simeq d^{-1}$, would change the above analysis and slightly compromise the applicability of the generalized RPA, as demonstrated in the Supporting Information.

The only unexplored assumption is that of the globule/macrophase internal homogeneity. To perform a stability analysis with respect to microphase separation, one should calculate the RPA spinodals by also taking into account short-range repulsive interactions. This interesting problem is beyond the scope of this work.

Other aspects neglected within the considered theoretical model and the following simulations are polymer−solvent dielectric (polarizability) mismatch and related solvation effects.[54,73−75,78,94−97] They become important at high polymer densities, when the dimensionless Bjerrum length u substantially depends on ϕ and should be accordingly renormalized.

We finally note that the extension of the developed framework to the salt-containing systems appears straightforward and should be performed in forthcoming publications.

IV. COLLAPSE OF POLYAMPHOLYTES OF DIFFERENT SEQUENCES

To describe the collapse of sequence-specific PAs induced by the increasing strength of Coulomb interactions, we use the Flory-type approach formulated by Birshtein and Pryamitsyn,[98] which was later refined by Grosberg and Kuznetsov.[99] Chain size is described by the dimensionless swelling ratio

$$\alpha = \frac{R_g}{R_g^{\text{id}}} \tag{43}$$

where R_g is the equilibrium radius of gyration, and $R_g^{\text{id}} = a\sqrt{N}/\sqrt{6}$ is that for the ideal-coil state. The free energy of the PA chain

$$\mathcal{F} = \mathcal{F}_{\text{conf}} + \mathcal{F}_{\text{Coul}} + \mathcal{F}_{\text{vol}} \tag{44}$$

consists of three terms responsible for (i) the conformational entropy, (ii) Coulomb correlation attractions, and (iii) short-range excluded volume repulsions. The entropic term is written as an interpolation between the regimes of swollen and collapsed PA[99]

$$\mathcal{F}_{\text{conf}} = \frac{9}{4}(\alpha^2 + \alpha^{-2}) \tag{45}$$

which takes the minimal value at $\alpha = 1$ in the ideal-coil state. The second term is given by

$$\mathcal{F}_{\text{Coul}} = \frac{V}{a^3}F_{\text{RPA}} = \frac{4\pi}{3}\left(\frac{5}{3}\right)^{3/2}\left(\frac{R_g}{a}\right)^3 F_{\text{RPA}} \tag{46}$$

Here we have used the relationship $R_g/R = \sqrt{3/5}$ between the radius of gyration and the geometrical radius in the globular state.[99] F_{RPA} is given by eqs 21 and 23−24, which were derived for the sequences considered in the previous

https://doi.org/10.1021/acs.macromol.2c00569
Macromolecules 2022, 55, 6260−6274

section. The third contribution, due to short-range repulsions, can be calculated in a similar way, $\mathcal{F}_{vol} = VF_{vol}/a^3$.

After several simple transformations invoking $\alpha^3 = t^3/N^{1/2}\phi$ closure with $t^3 = 81/5\sqrt{10}\pi$ and minimization of $\mathcal{F}$ with respect to the globule density ϕ, one arrives at an equation that expresses the balance of osmotic pressures

$$\pi_{vol} + \pi_{RPA} - \frac{3t^2}{2N^{4/3}}\phi^{1/3} + \frac{3}{2N^{2/3}t^2}\phi^{5/3} = 0 \quad (47)$$

Here $\pi_{RPA} = \phi\cdot\partial F_{RPA}/\partial\phi - F_{RPA}$ and

$$\pi_{vol} = \phi\frac{\partial F_{vol}}{\partial\phi} - F_{vol} = \frac{6\eta}{\pi}\left[\frac{1+\eta+\eta^2-\eta^3}{(1-\eta)^3} - 1 - 4\eta\right] \quad (48)$$

with $\eta = \pi\phi/6$ equal to the dimensionless packing fraction (volume fraction) of the monomers. Here we have assumed that the diameter of the spherical monomer and the polymer statistical segment are equal, $\sigma = a$. Equation 48 is the Carnahan−Starling (CS) result,[10,50,100−102] with the last term in the brackets subtracted to accommodate Θ solvent conditions, $\pi_{vol} \sim \eta^3$ for $\eta \to 0$. Another option would have been to use the Flory−Huggins expression with $\chi = 1/2$, but it strongly overestimates the globule's compressibility at high densities.

The resulting dependence of the PAs dimensions and densities on the strength of Coulomb interactions are shown in Figure 3. High clustering of opposite charges facilitates the early onset of the PA contraction, continuous shrinking, and a high density in the resulting globule. Figure 4 shows that in the regime of weak charge correlations PA dimensions approximately follow the expected scaling laws[25]

$$\alpha \sim \begin{cases} u^{-2/3}, & \text{alternating} \\ u^{-1/3}, & \text{ideally random} \\ u^{-1/9}, & \text{diblock} \end{cases} \quad (49)$$

that stem from eqs 31−33. These slopes are obtained within the so-called volume approximation, neglecting the conformational entropy and/or the surface energy of the globule.[99,103] The collapse of alternating PAs resembles that of a neutral polymer in a poor solvent (see section II.1), with a distinctive deviation from the volume approximation scaling in the early stages of the collapse.[99,103] The scaling given by eq 49 works the best for diblock PAs and less well for alternating PAs, as seen in Figure 4. This is because of the different u-width of the regime of weakly correlated globules for different sequences:[25] $(fN)^{1/4}$ for alternating, $(fN)^{1/2}$ for ideally random, and $(fN)^{3/2}$ for diblock PAs. Here we refer our earlier work[25] and eq 60 herein for a detailed discussion.

When charge correlations become strong, the swelling ratios of different PAs start to deviate from the scaling laws (49) but they approach each other, and so do the globule densities. This behavior is consistent with the universal, sequence-independent scaling picture of strongly correlated PA globules shown in Figure 1. Because short-range repulsions within the dense globule (which we describe by eq 48) do not follow any power law, no scaling power law is expected for the swelling ratio α.

One can, however, inspect the theoretical scaling for the energy of Coulomb interactions within the globule (eq 34). To this end, in Figure 5, we plot the corresponding free energy

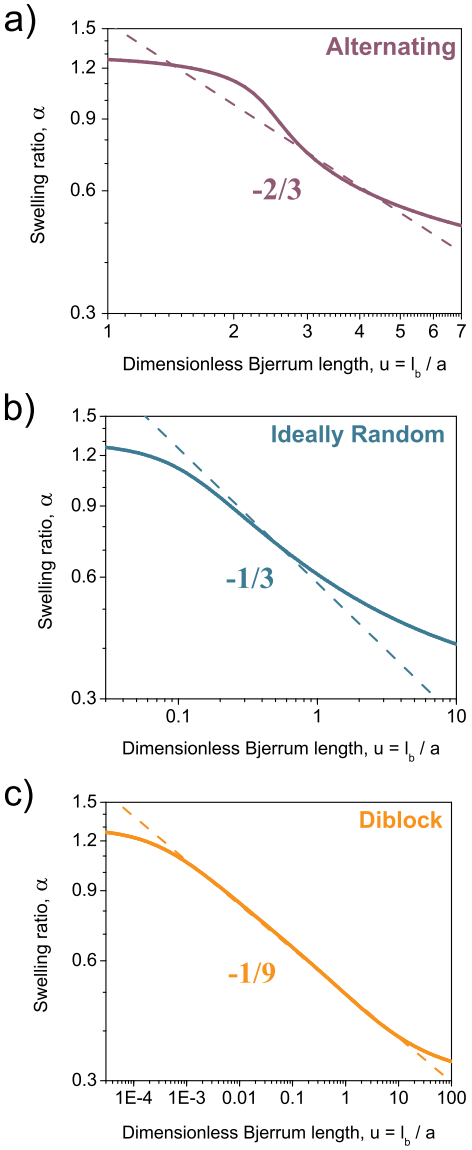

Figure 4. Swelling ratios of (a) alternating, (b) ideally random, and (c) diblock PAs in Θ solvent in the regime of weak charge correlations. The respective scaling laws derived within the volume approximation are shown with the dashed lines. PAs are fully charged, $f = 1$, and consist of $N = 10^3$ monomers.

density $\tilde{F}_{RPA}$ with the reference state being the system of disjointed charges, as discussed in section III.3. $\tilde{F}_{RPA}$ decreases with increasing Bjerrum length. It is the lowest for a diblock PA because of the higher density of its globule, and it is the highest for the most swollen alternating chain. The inset shows that the limiting strong-correlations law $\tilde{F}^{SC}_{RPA}/u\phi^{4/3} \approx -(9/\pi)^{1/3} \approx -1.42$ is fulfilled with reasonable accuracy for all types of sequences at $u \gtrsim 10$.

In the limit of weak Coulomb interactions, PAs have ideal-coil conformations. Here $\tilde{F}_{RPA}$ is low, and it coincides with their self-energy: $\tilde{F}^{db}_{RPA}/u\phi^{4/3} > 0$, $\tilde{F}^{alt}_{RPA}/u\phi^{4/3} < 0$, and $\tilde{F}^{rand}_{RPA}/u\phi^{4/3} \to 0$ at $u \to 0$. These results correspond to the positive, negative, and zero self-energies of diblock, alternating, and random PAs.[40,83]

https://doi.org/10.1021/acs.macromol.2c00569
Macromolecules 2022, 55, 6260−6274

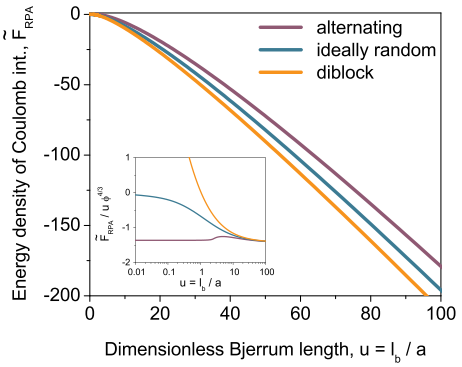

Figure 5. Density of the free energy of Coulomb interactions within a PA chain $\tilde{F}_{RPA}$ as a function of the dimensionless Bjerrum length u. The free energy reference level is the system of disjointed pointlike charges; i.e., $\tilde{F}_{RPA}$ contains the contribution due to the PA self-energy. The inset shows the dependence of $\tilde{F}_{RPA}/u\phi^{4/3}$ on u. Curves correspond to Θ solvent conditions, $N = 10^3$, and $f = 1$.

V. COMPUTER SIMULATIONS

The validity of our theoretical predictions is assessed by comparing them to results of coarse-grained (CG) molecular dynamics simulations of chain collapse for single-chain PAs. Simulations are performed with the LAMMPS package.[104] The Kremer−Grest model[105] is augmented with Coulomb interactions to consider alternating, ideally random, and diblock copolymers.[25] The connectivity of the monomers is provided by a FENE potential with $K = 30k_BT/\sigma^2$ and $R_0 = 1.5\sigma$, and all monomers interact via the Lennard-Jones (LJ) potential. The LJ parameter between all nonbonded monomers is $\varepsilon_{LJ} = 0.30k_BT$, and the cutoff distance is $R_c = 2.5\sigma$ to create Θ solvent conditions.[45] The strength of Coulomb interactions is controlled by the Bjerrum length; the range of $10^{-6} \leq l_b/\sigma \leq 32$ is studied here. To assess the reliability of our results at high Bjerrum lengths, for each chain statistics and l_b value, we performed at least two simulation runs starting from substantially different PA conformations, typically, a fully extended rodlike and a compact globular obtained at lower l_b. The state is considered to be at equilibrium if the same value of R_g (within the statistic error) is obtained for all initial configurations of the chain. Owing to this procedure of generating reproducible results, for diblock PAs, we were limited to $l_b/\sigma \leq 12$. For higher l_b, diblock PA globules are essentially frozen in, and the final R_g depends on the starting conformation of the PA; these nonequilibrium results are not shown in what follows. We note that 1−2 electrostatic interactions between adjacent bonded monomers are turned off to maintain the bond length, but *the corresponding energy is taken into account* (using post-analysis with pseudo-simulation runs) when the Coulomb energy W per one charged monomer is calculated. Additional simulation details can be found in ref 25.

The simulated dependence of R_g for all PAs, normalized by the value R_g^0 in the absence of Coulomb interactions, is shown with dots in Figure 6a. The simulation results are consistent with our theoretical expectations. Figure 6b−d shows that the predicted scaling laws for the PA globule size in the regime of

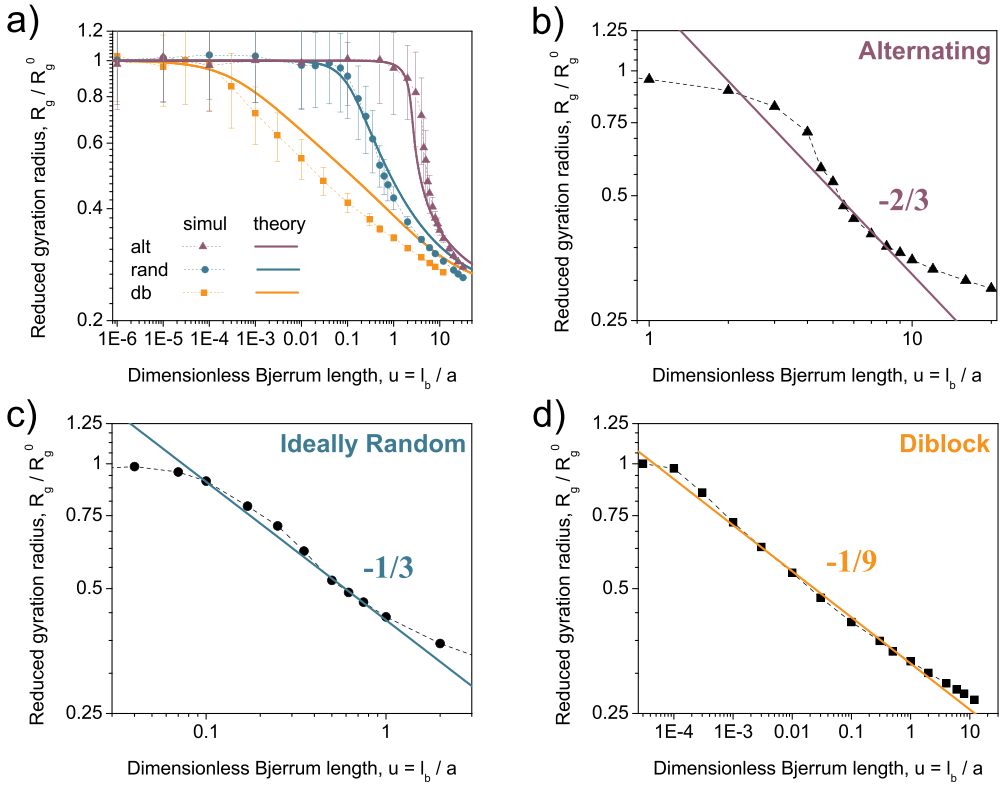

Figure 6. (a) Collapse of PAs with different sequences in Θ solvent. Simulations (dots) were performed for fully charged PAs, $f = 1$, containing $N = 1024$ monomers. The value of the radius of gyration in the absence of Coulomb interactions is $R_g^0 = 18.2 \pm 4.4$. The error bars are equal to the standard deviations and highlight the fluctuation regime of the PA. Theoretical curves (solid lines) are calculated for $N = 10^3$ and $f = 1$. (b−d) Comparison between simulation data (dots) and scaling laws (solid lines) in the regime of weak charge correlations for each of the PA sequences considered here.

https://doi.org/10.1021/acs.macromol.2c00569
Macromolecules 2022, 55, 6260−6274

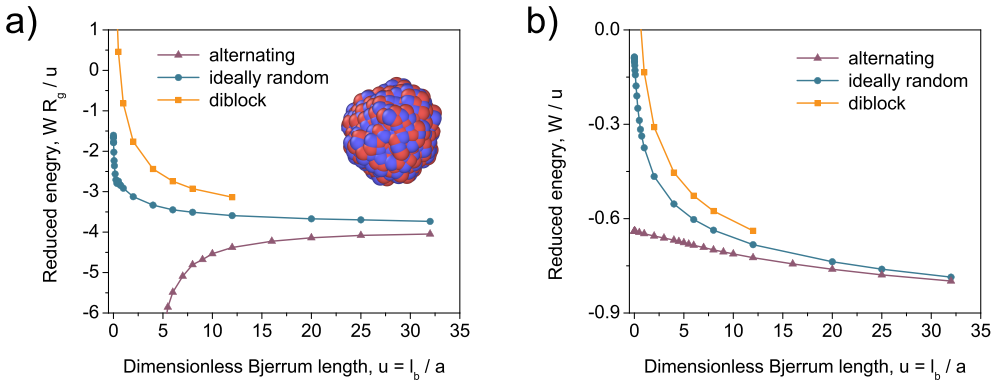

Figure 7. Reduced energies of Coulomb interactions per charge WR_g/u (a) and W/u (b). According to the Wigner liquid and ion-pairing theoretical models, the values of WR_g/u and W/u, respectively, should be independent of u in the regime of strong charge correlations, $u \gg 1$. The snapshot shown here depicts the structure of the strongly correlated globule of a random PA at $u = 32$.

weak correlations are well reproduced. Note that these scaling laws were also confirmed in our earlier work[25] within another simulation model, serving to highlight the universality of the power laws given by eq 49.

A quantitative comparison with the theory developed in section V can be achieved by plotting (Figure 6) the theoretical values of R_g/R_g^0. They differ from the swelling ratio α shown in Figure 4 because the latter was calculated with respect to the ideal-coil state and exceeds unity for $u \to 0$. This swelling of the (neutral) polymer chain at the Θ point—a point where the second virial coefficient vanishes—is due to the three-body and higher-order repulsions,[103,106] which are taken into account by the modified CS expression (eq 48).

The agreement between simulations and theory is reasonable over the entire range of Bjerrum lengths considered here. Theory predicts higher dimensions for the PAs at very high u because of the underestimation of the globule compressibility. In simulations, monomers are modeled by soft LJ particles, while the modified CS approach approximates them by hard spheres. Another inaccuracy is the assumption of equality between the monomer size and the statistical segment length, $\sigma = a$. In fact, within the KG model, the latter is twice as large as the former.[107] The modification of the RPA charge structure factors to account for the local rodlike chain conformations is straightforward[40] but would not enable derivation of closed-form results for the correlation free energies.

Because the osmotic pressure of repulsive interactions defined by eq 48 does not follow any power law at high densities, the theoretical scaling for $\tilde{F}_{RPA}$ in the regime of strong correlations cannot be corroborated by the R_g/R_g^0 dependence. For this reason, the (internal) energy of Coulomb interactions per charged monomer W has been directly calculated in simulations.[68] (In the regime of strong correlations, free energy and internal energy asymptotically coincide.) Figure 7a shows the reduced energy of Coulomb interactions, WR_g/u. At low u values, it is positive for diblock PAs and negative for alternating PAs and tends to zero for random chains, in accordance with the theoretical expectations shown in the inset of Figure 5. At high u, when Coulomb interactions are strong, the reduced energies are very close. If the Wigner liquid scaling $\tilde{F}_{RPA} = f\phi W \approx F_{RPA}^{SC} \simeq -u(f\phi)^{4/3}$ is correct, the ratio

$$\frac{WR_g}{u} = -\sqrt{\frac{3}{5}}\left(\frac{27fN}{4\pi^2}\right)^{1/3} \tag{50}$$

is independent of u and of the monomer sequence for $u \gg 1$. Figure 7a illustrates that this is indeed the case. The reduced energy rapidly reaches a plateau for all PAs considered in our simulations, $WR_g/u \approx -3.5 \pm 0.5$ in the regime of high Bjerrum lengths.

The value $WR_g/u = -6.88$ predicted by theory, which is found by substituting $f = 1$ and $N = 1024$ into eq 50, is noticeably lower. This discrepancy is due to the neglected role of the globule surface, that is, the volume approximation implied by the theoretical estimate. In fact, each surface charge has a 2 times lower number of neighbors and hence half (absolute value of) the energy of Coulomb interactions. The random PA globule that forms at $u = 32$ is shown in Figure 6a; it has $R_g = 4.75\sigma$ and a geometrical radius $R = \sqrt{5/3}\,R_g = 6.13\sigma$. The resulting globule area $A = 4\pi R^2 \approx 470\sigma^2$ suggests that nearly half of the monomer is at the surface, and $WR_g/u \approx -6.88 \times 0.75 = -5.16$ should be expected in simulations. This estimate is within 30% of the actual value and confirms the accuracy of the derived F_{RPA} in the limit of strong correlations. Moreover, eq 34 was derived under the assumption that the charges are connected by flexible Gaussian threads, which does not diminish the number of degrees of freedom, that is, three per monomer. In simulations, FENE bonds with $K = 30k_BT/\sigma^3$ are remarkably stiff and vibrations of the bond length are weak and negligible, so that each charge may effectively have only 2 degrees of freedom. If so, substituting $3 \to 2$ in the right-hand side of eq 19 yields $q_0^{bond} = (6\pi^2 f\phi)^{1/3}a^{-1}$ and

$$F_{RPA}^{SC,bond} = -\left(\frac{6}{\pi}\right)^{1/3} u(f\phi)^{4/3} = 0.87F_{RPA}^{SC} \tag{51}$$

This improves the theoretical estimate further, $WR_g/u \approx -5.16 \times 0.87 = -4.49$, leading to an accuracy of about 20%. The numerical agreement is reminiscent of the high accuracy of the RPA with the integration cutoff for the strongly correlated OCP.[64,87] The remaining discrepancy can be partially attributed to the approximate, asymptotic equality between the free energy of Coulomb interactions found theoretically and their internal energy obtained in simulations. More rigorous tests of the predicted numerical coefficient could be performed via simulations of macroscopic (self-)coacervate

https://doi.org/10.1021/acs.macromol.2c00569
Macromolecules 2022, 55, 6260−6274

phases and comparing the results to the theoretical internal energy of electrostatic interactions. The latter can be found from the free energy, for example, by using a Legendre transform.[2]

Finally, Figure 7b shows the values of W/u, which should be independent of u if the model of ion pairing and formation of the dipoles of fixed size was valid. One can see that W/u decreases substantially, even at very high u values, when $|\Delta E_{ip}| \gg 1$ and all monomers should form ion pairs. This continuous decrease in W/u is caused by the decreasing distance between nearest charges. The concerns raised earlier regarding pairwise ion association models in the context of strongly charged PAs are illustrated by the image showing a dense PA globule in Figure 7a. Every ionic monomer, even at the globule surface, is surrounded by approximately 5−7 surface counterparts as well as some others from the globule bulk. This correlation picture corresponds to the Wigner liquid representation sketched in Figure 1.

In summary, simulations confirm the limiting power laws derived here for weak and strong correlations. Furthermore, their agreement with theoretical results demonstrates that the generalized RPA with the q cutoff is nearly quantitative for strong charge correlations.

VI. CONCLUSION

The random phase approximation (RPA) has been extended to strong charge correlations, thereby providing a method to describe the equilibrium structure and thermodynamics of ionic assemblies such as polyampholyte and IDP globules, their self-coacervates, and complex coacervates of oppositely charged polyelectrolytes. The generalization of the RPA was achieved by (i) taking into account the pointlike nature of charges in polyampholyte or polyelectrolyte chains and by (ii) introducing an ultraviolet wavevector cutoff into the integration over the charge density fluctuations. The second aspect is sensitive to the microscopic detail of the polymer model, such as the chain stiffness and the type of the bond between the monomers, which define the number of independent degrees of freedom in the system. The proposed theoretical framework uniquely combines all of the following four features, which are not simultaneously available in other treatments of charge correlations in ion-containing polymeric systems:

(1) It is microscopic, does not rely on adjustable parameters, and is based on first-principles field-theoretic calculations of the Gaussian fluctuation correction to the (zero) mean-field free energy.

(2) It retains the advantages of the standard RPA, such as a consideration of polymer chain architecture, stiffness, conformational statistics, and distribution (sequence) of positively/negatively charged and neutral monomers.

(3) It is *rigorously valid* in the regime of strong charge correlations and is in quantitative agreement with results from simulations. At the scaling level of accuracy, it is consistent with results for the strongly correlated Wigner liquid (WL), the one-component plasma (OCP) model, and the high-density limit of the mean spherical approximation (MSA) in the liquid state theory (LST) for simple electrolytes.

(4) It provides the correlation free energies in closed, analytical form; this enables simple calculations that do not rely on numerical solution of the integral equations required within the LST and PRISM frameworks.

One limitation of the proposed approach is it is not applicable to spatially inhomogeneous systems. However, violations from homogeneity are only expected in the special case of low content of ionic monomers, $f \ll 1$, and simultaneous strong attractions, $u \gg 1$ (that is, for ionomer-type systems).

The theory introduced here has been applied to describe coil-to-globule transitions in polyampholytes with alternating, random, and diblock sequences of opposite charges. Coarse-grained computer simulations of polyampholyte collapse were performed to corroborate key and universal theoretical predictions. In the regime of weak correlations, when monomer sequence is critical, the scaling laws for the size of alternating/random/diblock PA globules are reproduced in simulations. In the regime of strong charge correlations, our theoretical result for the energy of Coulomb interactions has also been confirmed, with reasonable numerical agreement between theory and simulations. This agreement highlights the applicability of our approach to single-chain IDPs[108−110] and their self-coacervates[27]—systems where the precise description of the crossover region between weak and strong charge correlations is desired.

We believe that the key ideas of the proposed framework—(i) incorporation of the pointlike nature of charges into the charge structure factors and (ii) considering only physically meaningful fluctuations of the charge density field—may also be helpful for the improvement of other field-theoretic methods, such as the renormalized Gaussian fluctuation (RGF) theory by Wang et al. and the field-theoretic simulations (FTS) by Fredrickson et al. These methods are generically more accurate than the standard, nongeneralized RPA but, in their current form, are only applicable to weakly correlated systems. We emphasize that aspects i and ii are aimed at providing a consistent *formulation* of the particle-based problem in terms of the fluctuating fields, that is, proper particle-to-field transformations. Therefore, they are universal and independent of whether the formulated field-theoretic problem is *thereafter solved* approximately, as within the RPA and RGF, or exactly, as when FTS is employed.[111]

■ ASSOCIATED CONTENT

Supporting Information

The Supporting Information is available free of charge at https://pubs.acs.org/doi/10.1021/acs.macromol.2c00569.

(I) Description of the polyampholyte collapse: comparison between the generalized RPA and the standard RPA; (II) Discussion on the integration cutoff due to hard-core repulsions, $\tilde{q}_0 = a^{-1}$ (PDF)

■ AUTHOR INFORMATION

Corresponding Authors

Artem M. Rumyantsev − *Pritzker School of Molecular Engineering, University of Chicago, Chicago, Illinois 60637, United States;* orcid.org/0000-0002-0339-2375; Email: rumyantsev@uchicago.edu

Albert Johner − *Institut Charles Sadron, Université de Strasbourg, CNRS UPR22, Strasbourg 67034, France;* Email: albert.johner@ics-cnrs.unistra.fr

Juan J. de Pablo − *Pritzker School of Molecular Engineering, University of Chicago, Chicago, Illinois 60637, United*

https://doi.org/10.1021/acs.macromol.2c00569
Macromolecules 2022, 55, 6260−6274

States; orcid.org/0000-0002-3526-516X;
Email: depablo@uchicago.edu

Author

Matthew V. Tirrell − *Pritzker School of Molecular Engineering, University of Chicago, Chicago, Illinois 60637, United States;* orcid.org/0000-0001-6185-119X

Complete contact information is available at:
https://pubs.acs.org/10.1021/acs.macromol.2c00569

Notes

The authors declare no competing financial interest.

■ ACKNOWLEDGMENTS

A.M.R. gratefully acknowledges Nikolai Brilliantov for bringing ref 64 to his attention and Heyi Liang for many helpful comments related to the simulation aspects of this work. We are grateful to Jörg Baschnagel, Oleg Borisov, and Alexander Semenov for their valuable remarks. The authors also thank Angelika Neitzel, Heyi Liang, and Nicholas Jackson for many inspiring discussions. This work was supported by the Department of Energy, Office of Basic Energy Sciences, Division of Materials Science and Engineering.

■ REFERENCES

(1) Debye, P.; Hückel, E. Zur Theorie der Elektrolyte. *Phys. Z.* **1923**, *24*, 185−206.
(2) Landau, L. D.; Lifshitz, E. M. *Statistical Physics: Part 1*; Pergamon Press: New York, 1970.
(3) Fisher, M. E.; Levin, Y. Criticality in ionic fluids: Debye-Hückel theory, Bjerrum, and beyond. *Phys. Rev. Lett.* **1993**, *71*, 3826−3829.
(4) Luijten, E.; Fisher, M. E.; Panagiotopoulos, A. Z. Universality class of criticality in the restricted primitive model electrolyte. *Phys. Rev. Lett.* **2002**, *88*, 185701.
(5) Waisman, E.; Lebowitz, L. J. Mean spherical model integral equation for charged hard spheres I. Method of solution. *J. Chem. Phys.* **1972**, *56*, 3086−3093.
(6) Waisman, E.; Lebowitz, L. J. Mean spherical model integral equation for charged hard spheres. II. Results. *J. Chem. Phys.* **1972**, *56*, 3093−3099.
(7) Baus, M.; Hansen, J.-P. Statistical mechanics of simple Coulomb systems. *Phys. Rep.* **1980**, *59*, 1−94.
(8) Ichimaru, S.; Iyetomi, H.; Tanaka, S. Statistical physics of dense plasmas: Thermodynamics, transport coefficients and dynamic correlations. *Phys. Rep.* **1987**, *149*, 91−205.
(9) Levin, Y. Electrostatic correlations: From plasma to biology. *Rep. Prog. Phys.* **2002**, *65*, 1577−1632.
(10) Hansen, J. P.; McDonald, I. R. *Theory of Simple Liquids*; Academic Press: 2013.
(11) Sing, C. E.; Perry, S. L. Recent progress in the science of complex coacervation. *Soft Matter* **2020**, *16*, 2885−2914.
(12) Rumyantsev, A. M.; Jackson, N. E.; de Pablo, J. J. Polyelectrolyte complex coacervates: Recent developments and new frontiers. *Annu. Rev. Condens. Matter Phys.* **2021**, *12*, 155−176.
(13) Dinic, J.; Marciel, A. B.; Tirrell, M. V. Polyampholyte physics: Liquid-liquid phase separation and biological condensates. *Curr. Opin. Colloid Interface Sci.* **2021**, *54*, 101457.
(14) Brangwynne, C. P.; Tompa, P.; Pappu, R. V. Polymer physics of intracellular phase transitions. *Nat. Phys.* **2015**, *11*, 899−904.
(15) Aumiller, W. M.; Keating, C. D. Phosphorylation-mediated RNA/peptide complex coacervation as a model for intracellular liquid organelles. *Nat. Chem.* **2016**, *8*, 129−137.
(16) Pak, C. W.; Kosno, M.; Holehouse, A. S.; Padrick, S. B.; Mittal, A.; Ali, R.; Yunus, A. A.; Liu, D. R.; Pappu, R. V.; Rosen, M. K. Sequence determinants of intracellular phase separation by complex coacervation of a disordered protein. *Mol. Cell* **2016**, *63*, 72−85.
(17) Uversky, V. N. Protein intrinsic disorder-based liquid-liquid phase transitions in biological systems: Complex coacervates and membrane-less organelles. *Adv. Colloid Interface Sci.* **2017**, *239*, 97−114.
(18) Lin, Y.-H.; Forman-Kay, J. D.; Chan, H. S. Theories for sequence-dependent phase behaviors of biomolecular condensates. *Biochemistry* **2018**, *57*, 2499−2508.
(19) Lin, Y. H.; Forman-Kay, J. D.; Chan, H. S. Sequence-specific polyampholyte phase separation in membraneless organelles. *Phys. Rev. Lett.* **2016**, *117*, 178101.
(20) Lin, Y.-H.; Song, J.; Forman-Kay, J. D.; Chan, H. S. Random-phase-approximation theory for sequence-dependent, biologically functional liquid-liquid phase separation of intrinsically disordered proteins. *J. Mol. Liq.* **2017**, *228*, 176−193.
(21) Lin, Y.-H.; Chan, H. S. Phase separation and single-chain compactness of charged disordered proteins are strongly correlated. *Biophys. J.* **2017**, *112*, 2043−2046.
(22) McCarty, J.; Delaney, K. T.; Danielsen, S. P. O.; Fredrickson, G. H.; Shea, J.-E. Complete phase diagram for liquid−liquid phase separation of intrinsically disordered proteins. *J. Phys. Chem. Lett.* **2019**, *10*, 1644−1652.
(23) Danielsen, S. P. O.; McCarty, J.; Shea, J.-E.; Delaney, K. T.; Fredrickson, G. H. Molecular design of self-coacervation phenomena in block polyampholytes. *Proc. Natl. Acad. Sci. U. S. A.* **2019**, *116*, 8224−8232.
(24) Madinya, J. J.; Chang, L.-W.; Perry, S. L.; Sing, C. E. Sequence-dependent self-coacervation in high charge-density polyampholytes. *Mol. Syst. Des. Eng.* **2020**, *5*, 632−644.
(25) Rumyantsev, A. M.; Jackson, N. E.; Johner, A.; de Pablo, J. J. Scaling theory of neutral sequence-specific polyampholytes. *Macromolecules* **2021**, *54*, 3232−3246.
(26) Rumyantsev, A. M.; Johner, A.; de Pablo, J. J. Sequence blockiness controls the structure of polyampholyte necklaces. *ACS Macro Lett.* **2021**, *10*, 1048−1054.
(27) Nott, T. J.; Petsalaki, E.; Farber, P.; Jervis, D.; Fussner, E.; Plochowietz, A.; Craggs, T. D.; Bazett-Jones, D. P.; Pawson, T.; Forman-Kay, J. D.; Baldwin, A. J. Phase transition of a disordered nuage protein generates environmentally responsive membraneless organelles. *Mol. Cell* **2015**, *57*, 936−947.
(28) Wittmer, J.; Johner, A.; Joanny, J.-F. Random and alternating polyampholytes. *Eur. Phys. Lett.* **1993**, *24*, 263−268.
(29) Borue, V. Yu.; Erukhimovich, I. YA. A statistical theory of weakly charged polyelectrolytes: Fluctuations, equation of state and microphase separation. *Macromolecules* **1988**, *21*, 3240−3249.
(30) Borue, V. Yu.; Erukhimovich, I. YA. A statistical theory of globular polyelectrolyte complexes. *Macromolecules* **1990**, *23*, 3625−3632.
(31) Khokhlov, A. R.; Khachaturian, K. A. On the theory of weakly charged polyelectrolytes. *Polymer* **1982**, *23*, 1742−1750.
(32) Qin, J.; de Pablo, J. J. Criticality and connectivity in macromolecular charge complexation. *Macromolecules* **2016**, *49*, 8789−8800.
(33) Rumyantsev, A. M.; Jackson, N. E.; Yu, B.; Ting, J. M.; Chen, W.; Tirrell, M. V.; de Pablo, J. J. Controlling complex coacervation via random polyelectrolyte sequences. *ACS Macro Lett.* **2019**, *8*, 1296−1302.
(34) Potemkin, I. I.; Limberger, R. E.; Kudlay, A. N.; Khokhlov, A. R. Rodlike polyelectrolyte solutions: Effect of the many-body Coulomb attraction of similarly charged molecules favoring weak nematic ordering at very small polymer concentration. *Phys. Rev. E* **2002**, *66*, 011802.
(35) Kumar, R.; Audus, D.; Fredrickson, G. H. Phase separation in symmetric mixtures of oppositely charged rodlike polyelectrolytes. *J. Phys. Chem. B* **2010**, *114*, 9956−9976.
(36) Rumyantsev, A. M.; de Pablo, J. J. Liquid crystalline and isotropic coacervates of semiflexible polyanions and flexible polycations. *Macromolecules* **2019**, *52*, 5140−5156.
(37) Shen, K.; Wang, Z.-G. Polyelectrolyte chain structure and solution phase behavior. *Macromolecules* **2018**, *51*, 1706−1717.

(38) Lee, J.; Popov, Y. O.; Fredrickson, G. H. Complex coacervation: A field theoretic simulation study of polyelectrolyte complexation. *J. Chem. Phys.* **2008**, *128*, 224908.
(39) Delaney, K. T.; Fredrickson, G. H. Theory of polyelectrolyte complexation — Complex coacervates are self-coacervates. *J. Chem. Phys.* **2017**, *146*, 224902.
(40) Shen, K.; Wang, Z.-G. Electrostatic correlations and the polyelectrolyte self energy. *J. Chem. Phys.* **2017**, *146*, 084901.
(41) Dobrynin, A. V.; Colby, R. H.; Rubinstein, M. Polyampholytes. *J. Polym. Sci. B: Polym. Phys.* **2004**, *42*, 3513−3538.
(42) Shusharina, N. P.; Zhulina, E. B.; Dobrynin, A. V.; Rubinstein, M. Scaling theory of diblock polyampholyte solutions. *Macromolecules* **2005**, *38*, 8870−8081.
(43) Wang, Z.; Rubinstein, M. Regimes of conformational transitions of a diblock polyampholyte. *Macromolecules* **2006**, *39*, 5897−5912.
(44) Rumyantsev, A. M.; Zhulina, E. B.; Borisov, O. V. Complex coacervate of weakly charged polyelectrolytes: Diagram of states. *Macromolecules* **2018**, *51*, 3788−3801.
(45) Rubinstein, M.; Liao, Q.; Panyukov, S. Structure of liquid coacervates formed by oppositely charged polyelectrolytes. *Macromolecules* **2018**, *51*, 9572−9588.
(46) Castelnovo, M.; Joanny, J.-F. Complexation between oppositely charged polyelectrolytes: Beyond the random phase approximation. *Eur. Phys. J. E* **2001**, *6*, 377−386.
(47) Perry, S. L.; Sing, C. E. PRISM-based theory of complex coacervation: Excluded volume versus chain correlation. *Macromolecules* **2015**, *48*, 5040−5053.
(48) Bernard, O.; Blum, L. Thermodynamics of a model for flexible polyelectrolytes in the binding mean spherical approximation. *J. Chem. Phys.* **2000**, *112*, 7227−7237.
(49) Jiang, J. W.; Blum, L.; Bernard, O.; Prausnitz, J. M. Thermodynamic properties and phase equilibria of charged hard sphere chain model for polyelectrolyte solutions. *Mol. Phys.* **2001**, *99*, 1121−1128.
(50) Zhang, P.; Alsaifi, N. M.; Wu, J.; Wang, Z.-G. Salting-out and salting-in of polyelectrolyte solutions: A liquid-state theory study. *Macromolecules* **2016**, *49*, 9720−9730.
(51) Zhang, P.; Alsaifi, N. M.; Wu, J.; Wang, Z.-G. Polyelectrolyte complex coacervation: Effects of concentration asymmetry. *J. Chem. Phys.* **2018**, *149*, 163303.
(52) Zhang, P.; Shen, K.; Alsaifi, N. M.; Wang, Z.-G. Salt partitioning in complex coacervation of symmetric polyelectrolytes. *Macromolecules* **2018**, *51*, 5586−5593.
(53) Lytle, T. K.; Sing, C. E. Transfer matrix theory of polymer complex coacervation. *Soft Matter* **2017**, *13*, 7001−7012.
(54) Moldakarimov, S. B.; Kramarenko, E. Yu.; Khokhlov, A. R.; Kudaibergenov, S. E. Formation of salt bonds in polyampholyte chains. *Macromol. Theory Simul.* **2001**, *10*, 780−788.
(55) Kudlay, A.; Ermoshkin, A. V.; Olvera de La Cruz, M. Complexation of oppositely charged polyelectrolytes: Effect of ion pair formation. *Macromolecules* **2004**, *37*, 9231−9241.
(56) Salehi, A.; Larson, R. G. A molecular thermodynamic model of complexation in mixtures of oppositely charged polyelectrolytes with explicit account of charge association/dissociation. *Macromolecules* **2016**, *49*, 9706−9719.
(57) Friedowitz, S.; Salehi, A.; Larson, R. G.; Qin, J. Role of electrostatic correlations in polyelectrolyte charge association. *J. Chem. Phys.* **2018**, *149*, 163335.
(58) Lou, J.; Friedowitz, S.; Qin, J.; Xia, Y. Tunable coacervation of well-defined homologous polyanions and polycations by local polarity. *ACS Cent. Sci.* **2019**, *5*, 549−557.
(59) Danielsen, S. P. O.; Panyukov, S.; Rubinstein, M. Ion pairing and the structure of gel coacervates. *Macromolecules* **2020**, *53*, 9420−9442.
(60) Schiessel, H.; Pincus, P. Counterion-condensation-induced collapse of highly charged polyelectrolytes. *Macromolecules* **1998**, *31*, 7953−7959.
(61) Higgs, P. G.; Joanny, J. Theory of polyampholyte solutions. *J. Chem. Phys.* **1991**, *94*, 1543−1554.
(62) Castelnovo, M.; Joanny, J.-F. Formation of polyelectrolyte multilayers. *Langmuir* **2000**, *16*, 7524−7532.
(63) Liao, Q.; Dobrynin, A. V.; Rubinstein, M. Counterion-correlation-induced attraction and necklace formation in polyelectrolyte solutions: Theory and simulations. *Macromolecules* **2006**, *39*, 1920−1938.
(64) Brilliantov, N. V. Accurate first-principle equation of state for the one-component plasma. *Contrib. Plasma Phys.* **1998**, *38*, 489−499.
(65) Shklovskii, B. I. Wigner crystal model of counterion induced bundle formation of rodlike polyelectrolytes. *Phys. Rev. Lett.* **1999**, *82*, 3268−3271.
(66) Grosberg, A. Y.; Nguyen, T. T.; Shklovskii, B. I. Colloquium: The physics of charge inversion in chemical and biological systems. *Rev. Mod. Phys.* **2002**, *74*, 329−345.
(67) Solis, F. J.; Olvera de la Cruz, M. Collapse of flexible polyelectrolytes in multivalent salt solutions. *J. Chem. Phys.* **2000**, *112*, 2030−2035.
(68) Tom, A. M.; Vemparala, S.; Rajesh, R.; Brilliantov, N. V. Mechanism of chain collapse of strongly charged polyelectrolytes. *Phys. Rev. Lett.* **2016**, *117*, 147801.
(69) Neitzel, A. E.; Fang, Y. N.; Yu, B.; Rumyantsev, A. M.; de Pablo, J. J.; Tirrell, M. V. Polyelectrolyte complex coacervation across a broad range of charge densities. *Macromolecules* **2021**, *54*, 6878−6890.
(70) Eisenberg, A. Clustering of ions in organic polymers. A theoretical approach. *Macromolecules* **1970**, *3*, 147−154.
(71) Nyrkova, I. A.; Khokhlov, A. R.; Doi, M. Microdomains in block copolymers and multiplets in ionomers: Parallels in behavior. *Macromolecules* **1993**, *26*, 3601−3610.
(72) Semenov, A. N.; Nyrkova, I. A.; Khokhlov, A. R. Polymers with strongly interacting groups: Theory for nonspherical multiplets. *Macromolecules* **1995**, *28*, 7491−7500.
(73) Khokhlov, A. R.; Kramarenko, E. Y. Polyelectrolyte/ionomer behavior in polymer gel collapse. *Macromol. Theory Simul* **1994**, *3*, 45−59.
(74) Kramarenko, E. Y.; Erukhimovich, I. Y.; Khokhlov, A. R. The influence of ion pair formation on the phase behavior of polyelectrolyte solutions. *Macromol. Theory Simul.* **2002**, *11*, 462−471.
(75) Rumyantsev, A. M.; Kramarenko, E. Yu. Two regions of microphase separation in ion-containing polymer solutions. *Soft Matter* **2017**, *13*, 6831−6844.
(76) Wittmer, J.; Johner, A.; Joanny, J.-F. Precipitation of polyelectrolytes in the presence of multivalent salts. *J. Phys. (Paris)* **1995**, *5*, 635−654.
(77) Ermoshkin, A. V.; Olvera de la Cruz, M. A modified random phase approximation of polyelectrolyte solutions. *Macromolecules* **2003**, *36*, 7824−7832.
(78) Muthukumar, M. Theory of counter-ion condensation on flexible polyelectrolytes: Adsorption mechanism. *J. Chem. Phys.* **2004**, *120*, 9343−9350.
(79) Shen, K.-H.; Fan, M.; Hall, L. M. Molecular dynamics simulations of ion-containing polymers using generic coarse-grained models. *Macromolecules* **2021**, *54*, 2031−2052.
(80) de Gennes, P. G. *Scaling Concepts in Polymer Physics*; Cornell University: Ithaca, NY, 1979.
(81) Fredrickson, G. H. *The Equilibrium Theory of Inhomogeneous Polymers;* Clarendon Press: Oxford, 2006.
(82) Potemkin, I. I.; Palyulin, V. V. Complexation of oppositely charged polyelectrolytes: Effect of discrete charge distribution along the chain. *Phys. Rev. E* **2010**, *81*, 041802.
(83) Rumyantsev, A. M.; Potemkin, I. I. Explicit description of complexation between oppositely charged polyelectrolytes as an advantage of the random phase approximation over the scaling approach. *Phys. Chem. Chem. Phys.* **2017**, *19*, 27580−27592.
(84) Debye, P. Zur Theorie der spezifischen Wärmen. *Ann. Phys.* **1912**, *344*, 789−839.

https://doi.org/10.1021/acs.macromol.2c00569
Macromolecules 2022, 55, 6260−6274

(85) Kittel, C. *Introduction to Solid State Physics;* Wiley: New York, 2005.
(86) Kakljugin, A. S. Correlation energy of a non-Debye plasma. *Teplofizika Visokih Temperatur* **1985**, *23*, 217−223.
(87) Moreira, A. G.; Netz, R. R. One-component-plasma: Going beyond Debye-Hückel. *Eur. Phys. J. D* **2000**, *8*, 145−149.
(88) Brilliantov, N. V.; Malinin, V. V.; Netz, R. R. Systematic field-theory for the hard-core one-component plasma. *Eur. Phys. J. D* **2002**, *18*, 339−345.
(89) Gordievskaya, Yu. D.; Budkov, Yu. A.; Kramarenko, E. Yu. An interplay of electrostatic and excluded volume interactions in the conformational Behavior of a dipolar chain: Theory and computer simulations. *Soft Matter* **2018**, *14*, 3232−3235.
(90) Bohm, D.; Pines, D. A collective description of electron interactions: III. Coulomb interactions in a degenerate electron gas. *Phys. Rev.* **1953**, *92*, 609−625.
(91) In ref 77, Ermoshikin and Olvera de la Cruz considered the concentration regime where the solution correlation length exceeds the electrostatic blob size, $\xi > \xi_e$. In that regime the PEs adopt non-ideal-coil, locally stretched (rodlike) conformations. These authors explained that Coulomb interactions cannot be linearized, and hence the RPA cannot be used on the length scales smaller than ξ, and modified the RPA by introducing the concentration-dependent cutoff, $\tilde{q}_0 \simeq \xi^{-1} \sim \phi^{1/2}$, which enabled the calculation of correct binodals for the PE solution. It was also shown that using Brilliantov's cutoff $q_0 \simeq d^{-1} \sim \phi^{1/3}$ instead of $\tilde{q}_0$ yields similar results, albeit $\tilde{q}_0$ was preferred because ξ is the most important length scale in PE solutions at low concentrations. However, this integration cutoff was not aimed at extending the RPA to the strong charge correlations, which was achieved by employing an ion-pairing framework.[77] The polymer concentrations considered in that work were lower than in the present work; here we focus on dense, condensed states/phases of ionic polymers. Using q_0 given by eq 20 provides the most rigorous generalization of the RPA. The advantages of this cutoff over that due to the hard-core repulsions, $\tilde{q}_0 \simeq a^{-1}$, are addresses in the Supporting Information.
(92) The omitted contribution arises from the self-energy term, $\int d^3q (r_p q)^{-4}$, and is divergent at $q \to 0$ because of the infinite diblock PA length, $N \to \infty$. It can be regularized by considering finite-length chains.[83] Irrespective of N, this contribution is linear in ϕ and therefore irrelevant.
(93) Moldakarimov, S.; Johner, A.; Joanny, J.-F. Charge relaxation in polyampholytes of various statistics. *Eur. Phys. J. E* **2003**, *10*, 303−318.
(94) Nakamura, I.; Shi, A.-C.; Wang, Z.-G. Ion solvation in liquid mixtures: Effects of solvent reorganization. *Phys. Rev. Lett.* **2012**, *109*, 257802.
(95) Grzetic, D. J.; Delaney, K. T.; Fredrickson, G. H. The effective χ parameter in polarizable polymeric systems: One-loop perturbation theory and field-theoretic simulations. *J. Chem. Phys.* **2018**, *148*, 204903.
(96) Kwon, H.-K.; Ma, B.; Olvera de la Cruz, M. Determining the regimes of dielectric mismatch and ionic correlation effects in ionomer blends. *Macromolecules* **2019**, *52*, 535−546.
(97) Kong, X.; Hou, K. J.-Y.; Qin, J. Weakening of solvation-induced ordering by composition fluctuation in salt-doped block polymers. *ACS Macro Lett.* **2021**, *10*, 545−550.
(98) Birshtein, T. M.; Pryamitsyn, V. A. Theory of the coil-globule transition. *Polym. Sci. U. S. S. R.* **1987**, *29*, 2039−2046.
(99) Grosberg, A. Yu.; Kuznetsov, D. V. Quantitative theory of the globule-to-coil transition. 1. Link density distribution in a globule and its radius of gyration. *Macromolecules* **1992**, *25*, 1970−1979.
(100) Carnahan, N. F.; Starling, K. E. Equation of state for nonattracting rigid spheres. *J. Chem. Phys.* **1969**, *51*, 635−636.
(101) For hard-sphere fluids, the Carnahan−Starling equation is applicable for $\eta < \eta_c \approx 0.55$,[102] until the crystallization onset. In polymer systems crystallization is hindered by monomer connectivity, and η_c is even higher.
(102) Zaccarelli, E.; Valeriani, C.; Sanz, E.; Poon, W. C. K.; Cates, M. E.; Pusey, P. N. Crystallization of hard-sphere glasses. *Phys. Rev. Lett.* **2009**, *103*, 135704.
(103) Grosberg, A. Yu.; Khokhlov, A. R. *Statistical Physics of Macromolecules*; AIP Press: New York, 1994.
(104) Plimpton, S. Fast parallel algorithms for short-range molecular dynamics. *J. Comput. Phys.* **1995**, *117*, 1−19.
(105) Kremer, K.; Grest, G. S. Dynamics of entangled linear polymer melts: A molecular-dynamics simulation. *J. Chem. Phys.* **1990**, *92*, 5057−5086.
(106) Zhang, P.; Alsaifi, N. M.; Wang, Z.-G. Revisiting the Θ point. *Macromolecules* **2020**, *53*, 10409−10420.
(107) Auhl, R.; Everaers, R.; Grest, G. S.; Kremer, K.; Plimpton, S. J. Equilibration of long chain polymer melts in computer simulations. *J. Chem. Phys.* **2003**, *119*, 12718−12728.
(108) Müller-Späth, S.; Soranno, A.; Hirschfeld, V.; Hofmann, H.; Rüegger, S.; Reymond, L.; Nettels, D.; Schuler, B. Charge interactions can dominate the dimensions of intrinsically disordered proteins. *Proc. Natl. Acad. Sci. U. S. A.* **2010**, *107*, 14609−14614.
(109) Hofmann, H.; Soranno, A.; Borgia, A.; Gast, K.; Nettels, D.; Schuler, B. Polymer scaling laws of unfolded and intrinsically disordered proteins quantified with single-molecule spectroscopy. *Proc. Natl. Acad. Sci. U. S. A.* **2012**, *109*, 16155−16160.
(110) Das, R. K.; Pappu, R. V. Conformations of intrinsically disordered proteins are influenced by linear sequence distributions of oppositely charged residues. *Proc. Natl. Acad. Sci. U. S. A.* **2013**, *110*, 13392−13397.
(111) A broad class of FTS use particles with a Gaussian-smeared charge density instead of pointlike charges to avoid the self-energy divergences. We expect that the aspect ii should remain relevant for these FTS. At least, the q_0 integration cutoff is necessary when considering strong correlations within the FTS, which converge to the results of the field theories with pointlike charges as the radius of the charge smearing tends to zero.

https://doi.org/10.1021/acs.macromol.2c00569
Macromolecules 2022, 55, 6260−6274